Oligoester-Derivatized (Semi-) Interpenetrating Polymer Networks as Nanostructured Precursors to Porous Materials with Tunable Porosity

D. Grande, Geraldine Rohman

Oligoester-Derivatized (Semi-) Interpenetrating Polymer Networks as Nanostructured Precursors to Porous Materials with Tunable Porosity

Daniel Grande[1,*] and Géraldine Rohman[2]

[1] *Institut de Chimie et des Matériaux Paris-Est (ICMPE), UMR 7182 CNRS – Université Paris-Est Créteil, 2, rue Henri Dunant, 94320 Thiais, France*

[2] *Laboratoire de Chimie, Structures, Propriétés de Biomatériaux et d'Agents Thérapeutiques (CSPBAT), UMR 7244 CNRS – Université Paris-Nord, 74, rue Marcel Cachin, 93017 Bobigny Cedex, France*

Submitted as an Original Article to *Chemistry Africa*

* Corresponding author: Dr. Daniel Grande
Phone: +33 (0)1.49.78.11.77
Fax: +33 (0)1.49.78.12.08
E-mail: grande@icmpe.cnrs.fr
ORCID iD : 0000-0002-9987-9961

Acknowledgments: The "Région Ile-de-France" is gratefully acknowledged for financial support through SESAME projects allowing for the purchase of SEM equipment. The authors are indebted to late Prof. Ph. Guérin, Prof. F. Lauprêtre and Dr. S. Boileau for fruitful discussions in the field of chemistry and physico-chemistry of (semi-)IPNs.

Abstract

Porous polymeric materials with tunable porosity can be engineered from oligoester-derivatized semi-Interpenetrating Polymer Networks (semi-IPNs) or IPNs, respectively composed of either uncrosslinked or crosslinked aliphatic oligoesters entangled in a stiff subnetwork. In this paper, miscellaneous polyester/poly(methyl methacrylate)-based semi-IPN and IPN systems are first prepared as precursors with varying structural parameters, especially the nature (*i.e.*, poly(D,L-lactide), poly(ε-caprolactone)) and the molar mass (*i.e*, from 560 to 3,700 g.mol^{-1}) of the oligoester precursor. (Nano)porous networks with defined porosity are then generated through two complementary routes. This original paper discusses the scope and limitations of both approaches and investigates the correlation between the structure and morphology of the generated networks and the porosity of the resulting porous materials. We demonstrate that the choice of the precursors with defined compatibility is of paramount significance in the length scale of phase separation associated with nanostructured networks aswell as in the porosity scale of (nano)porous materials derived therefrom. Indeed, we find that the quantitative extraction of uncrosslinked oligoesters from semi-IPNs allows for the elaboration of nanoporous networks with pore diameters lower than 150 nm, provided that a high miscibility between both partners in semi-IPN precursors is attained, *i.e.* when using the lower molar mass oligoester. Alternately, the total hydrolysis of the polyester subnetwork associated with IPNs offers more versatility, since nanoporous networks can be obtained with a pore size range of 20-150 nm, regardless of the oligoester nature and molar mass in IPN precursors.

Keywords: Aliphatic oligoesters; (Semi-)Interpenetrating Polymer Networks; Extraction; Hydrolysis; Porous materials; Structure-morphology relationships

1 Introduction

The design of functional porous polymeric materials has been the subject of widespread interest and intense research, as they are involved in a wide array of applications, *e.g.* monoliths for chromatographic techniques, separation membranes, interlayer dielectrics, high surface area catalytic supports, as well as size/shape-selective nanoreactors [1-9]. Besides the classical synthetic strategies that rely on the use of solvents or gases as porogens, original approaches with porogen templates, capable of inducing specific structural pores within the residual structures, have been developed [10,11]. These template-oriented routes are quite interesting, since a wide array of porous polymers with a well-defined porosity can be designed.

Resorting to (semi-)Interpenetrating Polymer Networks ((semi-)IPNs) as nanostructured precursors to engineer porous crosslinked materials has solely been studied by a few research teams [12-19]. While semi-IPNs are composed of uncrosslinked sub-chains entrapped in a polymer network, IPNs constitute an intimate combination of two independent sub-networks, at least one of which is synthesized in the immediate presence of the other [20-25]. Although IPNs do not generally lead to chain interpenetration at the molecular length scale, small domain sizes from tens to a few hundreds of nanometers can be obtained under synthetically controlled experimental conditions. The peculiar interlocking framework confers to IPNs a microphase-separated co-continuous morphology leading to their unique properties. The IPN morphology essentially depends on the compatibility of each partner (*i.e.*, thermodynamic factor) and the kinetics and mechanism associated with the formation of each sub-network (*i.e.*, kinetic parameters). Nevertheless, if the phase morphology may be varied with several parameters, it has been reported that the phase continuity is controlled by the partner volume fractions and a co-

continuous morphology is generally obtained with a 50/50 composition [21-23]. Moreover, when IPNs are synthesized by the sequential method, *i.e.* when each sub-network is obtained in two consecutive steps, the first sub-network generally constitutes the most continuous phase and its cross-linking density is an important parameter to control the IPN morphology, while the cross-linking density of the second sub-network has no significant effect [26]. Consequently, the order of the sub-network formation is crucial as different phase morphologies and properties may be obtained. When arising from the combination of two partners that exhibit a contrasted degradability under specific conditions, such complex polymer structures are particularly interesting since nanoporous networks can be generated through selective degradation methods [12-19]. In this regard, IPNs based on a hydrolyzable polyester, such as poly(D,L-lactide) (PLA) or poly(ε-caprolactone) (PCL), and a non-hydrolyzable polymer, such as poly(methyl methacrylate) (PMMA), can be considered as appropriate precursors.

Straightforward routes to porous cross-linked polymeric materials through the utilization of PLA/PMMA semi-IPNs or IPNs as precursors were previously developed [26,27]. Porous methacrylic networks were readily generated from the quantitative extraction of uncrosslinked PLA oligomers in semi-IPNs or they were engineered from the selective hydrolysis of PLA sub-network in IPNs. The scope and limitations of both systems for the generation of (meso)porous materials were investigated. The effect of the cross-linker nature and the cross-linking density of the PMMA sub-network on the domain sizes in the (semi-)IPN precursors, and the correlation with the pore sizes distributions in the porous materials derived therefrom, were carefully studied. Macro- to mesoporous networks were derived from semi-IPNs and the variation of pore sizes was attributed to the miscibility of both partners in semi-IPN precursors [27]. For IPN systems, the pore sizes were always smaller than 100 nm, regardless of the cross-linker nature and

concentration, which showed that the cross-linking density of the PMMA sub-network and the compatibility between both sub-networks had a relatively small impact on phase separation in IPN precursors [28].

In light of the scarcity of studies on porous materials derived from (semi-) IPN systems, we decided to get a better insight into the correlation between the morphology of the (semi-)IPN precursors and the pore sizes of the resulting porous methacrylic networks, and notably on the impact of the molecular features of the first sub-network generated during IPN synthesis (*i.e.* polyester partner). In the present paper, miscellaneous polyester/PMMA (semi-)IPNs with a 50/50 composition are prepared to ensure the co-continuity of each phase, and the effect of the nature and molar mass of the oligoester precursor is systematically investigated for the first time. In this regard, poly(D,L-lactide) (PLA) or poly(ε-caprolactone) (PCL) oligomers are used with different molar masses. We particularly pay attention to the correlations between the structure and morphology of the (semi-)IPN precursors and the porosity of the resulting porous materials through various physico-chemical analyses, since the control of the precursor miscibility associated with both types of reference systems is of paramount significance for the design of nanoporous materials with defined pore sizes.

2 Experimental

2.1 Materials

Dihydroxy-telechelic PLA oligomers were synthesized by ring-opening polymerization of D,L-lactide initiated by the ethylene glycol/tin (II) octanoate system, according to a literature method [29]. Dihydroxy-telechelic PCL oligomers were purchased from Aldrich. Dibutyltin dilaurate

(DBTDL, Fluka) was used as received. 4,4',4''-triisocyanato-triphenylmethane (Desmodur® RU; 1.25 mol.L^{-1} in dichloromethane solution) was provided by Bayer. Methyl methacrylate (MMA, Aldrich) was dried over CaH_2, and distilled under vacuum prior to use. Diurethane dimethacrylate (DUDMA) were purchased from Aldrich and used as received. AIBN (Merck) was purified by recrystallization in methanol.

2.2 Preparation of Precursory Networks

In all experiments, a mold was devised by clamping together two glass plates separated by a 2 mm-thick silicone rubber gasket.

2.2.1 Polyester Single Networks

Polyester single networks were prepared with a (Oligoester + Desmodur® RU)/dichloromethane mass composition of 50/50 wt% and ratios of $[NCO]_0/[OH]_0$ and $[DBTDL]_0/[Oligoester]_0$ equal to 1.4 and 0.44, respectively. An example of the preparation of a PLA single network is given hereafter. 1g of PLA (M_n = 1,700 g.mol^{-1}; 5.9×10^{-4} mol) was dissolved in 0.91mL of dichloromethane (1.21g), and subsequently, 0.45mL of Desmodur® RU (0.21g; 5.6×10^{-4} mol) and 0.15 mL of DBTDL (2.5×10^{-4} mol) were added. The solution was then poured into the mold and kept at room temperature for 20h. Thereafter, the mold was heated to 65°C for 2h, and then to 110°C for 2 h (**Fig. 1**).

2.2.2 PMMA Single Network

An example of the preparation of a single network with a MMA/DUDMA molar composition of 90/10 mol% is given hereafter. A mixture of MMA (0.9 g; 9×10^{-3} mol), DUDMA (0.47 g; 10^{-3} mol), and AIBN (0.033 g; 0.2×10^{-3} mol, $[AIBN]_0/([MMA]_0 + 2[DUDMA]_0) = 0.02$) was

degassed under vacuum, poured under nitrogen into the mold. Then, the mixture was heated at 65°C for 2h, and cured at 110°C for 2h (**Fig. 2**).

2.2.3 Oligoester/PMMA Semi-IPNs

An example of the preparation of a semi-IPN with a PLA/PMMA mass composition of 50/50 wt% and a MMA/DUDMA molar composition of 90/10 mol% ($[AIBN]_0/([MMA]_0 + 2[DUDMA]_0) = 0.02$) is given hereafter. 0.50g of PLA (M_n = 1,700 g.mol^{-1}; 2.9×10^{-4} mol), 0.33g of MMA (3.3×10^{-3} mol), 0.17 g of DUDMA (3.6×10^{-4} mol), and 12 mg of AIBN (7.3×10^{-5} mol) were mixed, degassed under vacuum, and poured into the mold under nitrogen. The system was then heated to 65°C for 2h, and cured at 110°C for a 2h (**Fig. 3**).

2.2.4 Polyester/PMMA IPNs

An example of the preparation of an IPN with a PLA/PMMA mass composition of 50/50 wt%, ratios of $[NCO]_0/[OH]_0$ and $[DBTDL]_0/[Oligoester]_0$ equal to 1.4 and 0.44, respectively, and a MMA/DUDMA molar composition of 90/10 mol% ($[AIBN]_0/([MMA]_0 + 2[DUDMA]_0) = 0.02$) is given hereafter. 1g of PLA (M_n = 1,700 g.mol^{-1}; 5.9×10^{-4} mol), 0.76 g of MMA (7.6×10^{-3} mol), 0.40 g of DUDMA (8.5×10^{-4} mol), and 27.7 mg of AIBN (1.7×10^{-4} mol) were mixed and degassed under vacuum. Then, 0.45mL of Desmodur® RU (0.21 g; 5.6×10^{-4} mol) and 0.15 mL of DBTDL (2.5×10^{-4} mol) were added under nitrogen, and the solution was poured into the mold and kept at room temperature for 20h.. Finally, the system was heated to 65°C for 2h, and cured at 110°C for 2h (**Fig. 4**).

Other single polyester networks and (semi-)IPNs were synthesized in similar ways by changing the nature and/or the molar mass of the oligoester precursor.

2.3 Extraction of Networks and Formation of Porous Networks from Semi-IPNs

All networks and (semi-)IPNs were Soxhlet extracted with dichloromethane for 24h at 40°C. After extraction, the samples were dried under vacuum, weighed, and the sol fractions (mass percentages of extractables) were calculated. The extraction of linear oligoesters from semi-IPNs led to the formation of residual porous PMMA networks (**Fig.3**).

2.4 Formation of Porous Networks by Partial Hydrolysis of IPNs

0.2 g of IPNs were immersed at 60°C in a mixture composed of 4 mL of a methylamine solution (pH = 13.6) and 4 mL of ethanol. After 24h, the residual networks were rinsed with deionized water up to neutral pH, and dried under vacuum. The mass loss (Δm) was assessed as follows (Equation 1):

$$\Delta m\ (\text{wt\%}) = 100 \times (m_0 - m_d)/m_0 \qquad (1)$$

where m_0 and m_d stand for the initial mass of the samples and their residual mass after vacuum drying, respectively.

The total hydrolysis of the polyester sub-network led to the formation of residual porous PMMA networks (**Fig.4**).

2.5 Instrumentation

FTIR spectra were recorded between 4,000 and 450 cm^{-1} by averaging 32 consecutive scans with a resolution of 4cm^{-1} on a Bruker Tensor 27 DTGS spectrometer in Attenuated Total Reflection (ATR) mode.

DSC thermograms were recorded with a Perkin Elmer DSC7 calorimeter under nitrogen atmosphere. The analyses were carried out at a heating rate of 20°C.min^{-1} and the second run was performed after quenching. In order to avoid network degradation during the analysis, PMMA

single networks and (semi-)IPNs were scanned twice from –100 to 200°C, while polyester single networks and oligoester precursors were scanned from –100 to 100°C and from –100 to 200°C for the first and second scans, respectively. The T_g ranges were measured in the second run through the determination of the values associated with the intercepts of tangent to midpoint of the specific heat increment with "glassy"(lower limit, $T_{g,onset}$) and "viscous" baselines (upper limit, $T_{g,end}$), respectively.

^{1}H and ^{13}C spectra of sol fractions and hydrolysis products were recorded at room temperature using a Bruker Avance II spectrometer operating at a resonance frequency of 400 and 100 MHz, respectively. The sample concentration was 10 $mg.mL^{-1}$, and $CDCl_3$ was used as the solvent and internal standard (7.27 ppm).

The Size Exclusion Chromatography (SEC) equipment comprised a Spectra Physics P100 pump, two PLgel 5 μm mixed-C columns (Polymer Laboratories), and a Shodex RI 71 refractive index detector. Tetrahydrofuran (THF) was used as the eluent at a flow rate of 1 $mL.min^{-1}$, and polystyrene standards (Polymer Laboratories) were employed for calibration.

Scanning Electron Microscopy (SEM) analyses were performed with a LEO 1530 microscope equipped with a high-vacuum (10^{-10} mmHg) Gemini column. The accelerating tensions ranged from 1 to 5 kV; two types of detectors (InLens and Secondary Electron) were used. Prior to analyses, the samples were cryofractured and coated with a Pd/Au alloy (4 nm) in a Cressington 208 HR sputter-coater.

2.6 Thermoporometry by DSC

The pore size and pore size distribution of the porous materials were determined through thermoporometry based on the melting temperature (T_m) depression of a liquid constrained within

the pores [30-32]. To this purpose, the samples were immersed in ethanol for 2h, and then placed for 1h in ethanol/water mixtures of various compositions (70/30, 50/50, 30/70 vol%). After a 2 week immersion in pure water, the melting thermograms of wiped samples were recorded from –50 to 5°C at a heating rate of 1 °C.min^{-1}.

The pore size distribution was obtained by plotting dV/dR *vs*. the pore diameter (D_p) evaluated by using Equation 2 and 3, respectively [30-32]:

$$dV/dR\ (cm^3.nm^{-1}.g^{-1}) = [(dq/dt)\times(T_m - T_{m0})^2] / [32.33\times\rho\times v\times m\times\Delta H(T)] \quad (2)$$

$$D_p\ (nm) = 2 \times [0.68 - 32.33/(T_m - T_{m0})] \quad (3)$$

where T_m and T_{m0} are the melting temperatures of confined and bulk water, respectively, and dq/dt, ρ, v, m and ΔH(T) are the heat flow recovered by DSC, the water density, the heating rate, the sample mass and the melting enthalpy of water, respectively. $\Delta H(T)$ was calculated from Equation 4 [30-32]:

$$\Delta H(T)\ (J.g^{-1}) = 332 + 1.39\times(T_m - T_{m0}) + 0.155\times(T_m - T_{m0})^2 \quad (4)$$

2.7 Determination of Density and Porosity Ratio Values

The samples were immersed in ethanol for 2h, and then placed for 1h in ethanol/water mixtures of various compositions (70/30, 50/50, 30/70 vol%). After a 2 week immersion in pure water, the wet mass was measured, and the mass swelling ratio (q_w), the pore volume (V_{pore}), and the apparent density (d_{app}) were calculated from Equation 5, 6 and 7, respectively [33]:

$$q_w = m_w/m_d \quad (5)$$

$$V_{pore}(cm^3.g^{-1}) = (q_w - 1)/d_s \quad (6)$$

$$V_{pore} = 1/d_{app} - 1/d_{true} \quad (7)$$

where m_w, m_d, d_s and d_{true} stand, respectively, for the samples wet mass , their mass after vacuum drying, the solvent density (water), and the true density of the PMMA matrix measured by helium pycnometry at 25°C by using A Micromeritics Accupyc 1330 equipment.

The porosity ratio P was then calculated by using Equation 8:

$$P = 1 - d_{app}/d_{true} \quad (8)$$

3 Results and Discussion

3.1 Preparation of Semi-IPN Precursors and Investigation of Phase Separation

Various Oligoester/PMMA (50/50 wt%) semi-IPNs were prepared by bulk free-radical copolymerization of MMA and DUDMA with a composition of 90/10 mol%, in the presence of oligoesters of different natures and molar masses (**Table 1**). The radical polymerization occurred at 65°C and the cross-linking completion arose during the final curing at 110°C (**Fig. 3**), which was confirmed by the absence of the C=C absorption band of MMA and dimethacrylate monomers at 1,640 cm^{-1} in the FTIR spectra. In a previous study concerning the kinetics of network formation, it was shown that "soft" oligoesters behaved like a diluent toward the methacrylic copolymerization process which led to the complete conversion of C=C bonds before the curing process [25]. Moreover, the kinetic process was not greatly affected by the variation of the polyester nature or molar mass (data not shown).

For (semi-)IPN-related materials [21,22], the turbidity τ, which corresponds to the relative attenuation of light by the materials, accounts for the degree of chain interpenetration and allows for the determination of the microdomain size, provided the difference between the refractive

indices of both partners is significant ($\Delta n \geq 0.02$). Indeed, microdomain sizes are smaller than about150 nm when materials are transparent, while the opaque ones possess microdomain sizes higher than 150 nm [34]. **Table 2** reports the different visual aspects observed for semi-IPNs before extraction. In the case of PLA-based semi-IPNs, the experimental n_D^{25} values measured for the PLA oligomer and a PMMA network were quite different ($n_D^{25}{}_{PLA} = 1.46$, $n_D^{25}{}_{PMMA} = 1.49$), and therefore the material turbidity can be used to evaluate the effect of the oligoester molar mass on the phase separation. It is noteworthy that the increase in the PLA molar mass led to an increase in the oligoester domain sizes, as semi-IPNs were transparent when the molar mass of the oligomer was equal to 570 g.mol^{-1} and opaque when the latter was equal to 3,700 g.mol^{-1}. For PCL-based semi-IPNs, the n_D^{25} values of PMMA sample and PCL oligomer ($n_D^{25}{}_{PCL} = 1.49$) were quite identical, and it was consequently difficult to take into account the transparency of the samples. Nevertheless, there was clearly a phase separation when the samples were opaque. Consequently, it was possible to conclude that PCL oligomers led to higher oligoester domain sizes compared to PLA oligomers with the same molar mass, as semi-IPNs were opaque with PCL 2,100 g.mol^{-1} and translucent for PLA 1,700 g.mol^{-1}.

Semi-IPN samples, before extraction,displayed single and fairly narrow glass transitionranges (**Table 2**).The T_g values were quite low but comprised between the T_g of corresponding oligoester (**Table 1**) andthat of PMMA single network (**Table 3**).Yet, theT_g ranges of semi-IPNs did not match the valuescalculated from the Fox equation for miscible blends.For PLA-based semi-IPNs, the transparent aspect of the samples solely argued in favor of the absence ofphase separation at a length scale of a few hundreds ofnanometers. Moreover, the values of the heat capacity jump at theglass transition (ΔC_p) decreasedwhen the molar mass of the PLA

oligomers increased and became smaller than the values obtained for a 50/50 wt% physical blend constituted of PLAoligomer and PMMApreparedunder experimental conditions identical tothose employed for single network preparation (ΔC_p = 0.33 J.g^{-1}.°C^{-1}). This result also corroborated the conclusionsinferred from the visual observations concerning the increase in phase separation when using oligomers with higher molar masses. In the case of PCL oligomers, the values of ΔC_p found for miscible blends were 0.18 and 0.28 J.g^{-1}.°C^{-1} for PCL 560 and 2,100 g.mol^{-1}, respectively. As a consequence, both PCL-containing semi-INPs exhibited a phase separation at the length scale of a few hundred nanometers. One more time, the phase separation was found higher for PCL-based semi-IPNs compared to PLA ones with the same molar mass as the differences between the values of ΔC_p for semi-IPNs and those for miscible blends increased. Finally, a decrease in the enthalpy of melting and inthe crystallinitydegree of PCL oligomers were observed in semi-IPNs as PMMA hindered the oligoester crystallization [34].

In a previous paper [24], we already related the dependence of domain size to the polymer-polymer miscibility in semi-IPN precursors, thanks to the calculation of PLA/PMMA interaction parameters (χ) and critical interaction parameters (χ_{cr}). We hypothesized that the domain sizes could be tuned by varying structural parameters through the variation of miscibility between the oligoester and the PMMA sub-network. In order to confirm this idea, we also evaluated these parameters in PLA/PMMA and PCL/PMMA semi-IPNsunder investigation, and we studied the effect of the variation of the oligoester molar mass. Because relatively weak interactions (van der Waals forces or hydrogen bonds) are involved in the systems under study, the χvalues could be related to the Hildebrand solubility parameters of both partners using Equation9 [35-38]:

$$\chi = \frac{V_m}{R \cdot T} \cdot (\delta_1 - \delta_2)^2 \qquad (9)$$

where V_m and $T$are the reference molar volume andthe temperature, taken as 100 $cm^3.mol^{-1}$ and 298 K,respectively, $R$is the gas constant, δ_1 is the solubilityparameter of oligoester, and δ_2 is the solubility parameter ofa methacrylic copolymer network.

δ_1 was calculatedusing the group contribution method based on VanKrevelen's molar attraction constants:[29] δ_1= 18.56± 0.15 $MPa^{1/2}$ for PLA and δ_1=17.94 ± 0.15 $MPa^{1/2}$ for PCL. δ_2 was calculatedusing an additive molar contribution relationship and was found to equal 20.76 ± 0.15 $MPa^{1/2}$ for a 90/10 mol% MMA/DUDMA network [26]. As a matter of fact, the values of χwere 0.19 ±0.05 and 032 ±0.07 for PLA/PMMA and PCL/PMMA semi-IPNs, respectively. As the χ value was higher for PCL-based systems, it could be concluded that PCL oligomers led to less miscibility with the PMMA sub-network in semi-IPN precursors. To evaluate the influence of oligoester molar masson the miscibility of both semi-IPN partners, χ_{cr} were estimated for thesystems considered. The χ_{cr} values were calculated fromEquation 10 [35-38]:

$$\chi_{cr} = \frac{1}{2}\cdot\left(\frac{1}{\sqrt{N_1}}+\frac{1}{\sqrt{N_2}}\right)^2 \qquad (10)$$

where N_1 and N_2 are the polymerization degrees of oligoester and PMMA sub-networks, respectively. Whena polymer is cross-linked, $N$is equal to infinity; hence,the latter equation could simply be expressed as follows(Equation 11):

$$\chi_{cr} = \frac{1}{2\cdot N_1} \qquad (11)$$

Applying Equation12 to the PLA and PCL oligomers used in thisinvestigation, the value of χ_{cr}could be calculated. Nevertheless, it should be stressed that these valuesare valid for systems withonly dispersive forces. According to Coleman's practicalguide to polymer miscibility [37],$\Delta\delta_{cr}$ can be increased bysteps of 0.25 $(cal.cm^{-3})^{1/2}$, depending on the strength ofthe potential

intermolecular interactions present betweenthe polymeric components of biphasic systems.In DUDMA-based semi-IPNs,hydrogen bonding could potentially be established betweenthe urethane functions of DUDMA cross-linksand the main-chain ester groups of oligoester. We previously demonstrated that theextent of hydrogen bonding, so in turn the strength ofintermolecular interactions, could be increased withincreasing amounts of DUDMA [26]. Therefore, $\Delta\delta_{cr}$ wasfurther increased depending on the DUDMA content.The initial$\Delta\delta_{cr}$ values were estimated for each oligoesters using the reference molar volume of 57.7 $cm^3.mol^{-1}$ and 106.5 $cm^3.mol^{-1}$for PLA and PCL, respectively. After the appropriate step increase for 10 mol% DUDMA-based systems [26],χ_{cr} values were calculated and are given in **Table 4**. Consequently, these values showed that the miscibility decreased when the oligoester molar mass increased as χ_{cr}became smaller. Finally, the limits of miscibility could be predicted from the difference χ_{cr}-χ. Indeed, when the value of χ_{cr}-χ> 0, the system can be considered to be miscible, while it is immiscible if χ_{cr}-χ< 0. Therefore, 10 mol% DUDMA-based semi-IPNs containing PLA 570 $g.mol^{-1}$ would not exhibit phase separation, while PLA 3,700 $g.mol^{-1}$ or PCL 2,100 $g.mol^{-1}$-based systems should. At least, PLA 1,700 and PCL 560 $g.mol^{-1}$-based systemswere in the limit of phase separation as the values of χ_{cr}-χwere around 0. To conclude, this theoretical approach may well account for the different behaviourstowards phase separation in semi-IPNs when varying the oligoester nature or molar mass. Indeed, thecalculation of oligoester/PMMA interaction parameters andthe comparison between $\chi$and χ_{cr} values corroborated the conclusions inferred from our previous results associated with DSC analysis and visual aspects.

3.2 Synthesis of IPN Precursors and Investigation of Microphase Separation

IPNs constituted of polyester and PMMA sub-networks (50/50 wt%) were synthesized by the *in situ* sequential method, *i.e.* by mixing all the precursors homogeneously, and then forming both networks *via* two successive and non-interfering cross-linking reactions. Hence, the polyestersub-network was first generated at room temperature for 20h by DBTDL-catalyzed cross-linking of dihydroxy-telechelic oligoesters(molecular characteristics described in **Table 1**) with a pluriisocyanate, *i.e.*Desmodur® RU. Subsequently, the methacrylic sub-network was created at 65°C (2h) by AIBN-initiated free-radical copolymerization of MMA and DUDMA with a molar ratio of 90/10, and finally cured at 110°C for 2h to ensure a near completion of the cross-linking processes (**Fig. 4**) [27,39,40].Next, the IPN samples were extracted in a Soxhlet device with CH_2Cl_2 for 24h, and the amounts of soluble fractions are reported in **Table 5**.The soluble fractions were always below 14 wt% which matched with the sum of the corresponding polyester and PMMA single networks soluble fractions, except for PLA 3,700 $g.mol^{-1}$-based IPNs in which soluble fractions were very high. In the latter case, the SEC analysis of the soluble fractions showed that they were constituted in majority of PLA oligomer precursors (around 85%). DBTDL, PMMA oligomers, and only traces of residual methacrylates were also found by ^1H NMR. On the contrary, a high ratio of PMMA with molar mass ranging from 100 to 60,000 $g.mol^{-1}$ was extracted from PLA 570 $g.mol^{-1}$-based IPNs, and a higher content of residual methacrylates was also found. However, the IRTF study of networks after extraction revealed that hydroxyl groups were still present in IPNs synthesized from oligoester with low molar mass which indicated that the cross-linking of polyester sub-network was not complete. The variations of the kinetic process of the polyester sub-network with the oligoester precursor molar masswerenot studied as the Lambert-Beer Law was not valid for low molar mass.

Concerning the PMMA-sub-network formation, we showed in a previous study [27] that the "soft" polyester sub-network acted as a diluent towards the methacrylic copolymerization process, preventing the reaction medium from attaining the glassy state as a solvent would have done it. However, as the free-radical polymerization proceeded, the T_g of the system increasedand the temperature of the reaction medium, *i.e.* 65°C, was around the T_g values of IPNs (**Table 6**). Therefore, the polymerization was considered to take place in a confined medium (into the polyester sub-network matrix) and was going to stop unless the temperature was increased to 110°C.We also found that the kinetic process was not greatly affected by the variation of the polyester nature or molar mass (data not shown).

Interestingly, all IPNs were transparent indicating that domain sizeswere always smaller than 150nm as the difference between the refractive indices ofboth sub-networkswas significant ($\Delta n \geq 0.02$). Actually, theexperimental n_D^{25} values measured for the PLA and PCL sub-networks were equal to 1.51 and 1.53, respectively, while that for PMMA sub-network was equal to 1.49.Such visual observations showed that chain interpenetration of both polyester and PMMA sub-networks in the interlocking configuration of IPNs led to a significant decrease in the phase separation compared to the corresponding semi-IPN homologues. This was particularly true for systems with a higher degree of immiscibility like those with PLA 3,700 $g.mol^{-1}$ and PCL 2,100 $g.mol^{-1}$ as the semi-IPNs synthesized with these oligomers were opaque.

DSC analyses also confirmed the decrease in phase separation in IPNs (**Table 6**). Indeed, all IPNs displayed single glass transition ranges comprised between the T_g of corresponding polyester sub-networks and that of PMMA single network (see **Table 3**), which argued in favor of the absence of phase separation at a length scale of a few hundreds of nanometers. No melting temperatures were detected in PCL-based IPNs, as the oligoester cross-linking totally prevented

PCL crystallization. Moreover, the values of the heat capacity jump at the glass transition (ΔC_p) were always equalor close to the expected ΔC_pvalue of a 50/50 wt% physical blend theoretically constituted of polyester and PMMA networks($\Delta C_{p,theoretical}$ = 0.25 $J.g^{-1}.°C^{-1}$), except for PCL 2,100 $g.mol^{-1}$-based IPNs. Nevertheless, the ΔC_p values decreased when the oligoester precursor molar mass increasedshowing that the domain sizes were still higher for these systems,like in the case of semi-IPN systems. This was very clear when using PCL 2,100 $g.mol^{-1}$ as the value of $\Delta C_p$was equal to only 0.14 $J.g^{-1}.{}^oC^{-1}$. This trend was also supportedby the increase inΔT_g with the oligoester precursor molar mass.All these results confirmed that the phase separation in IPNs was mainly governed by the interpenetration created by the cross-linking of both partners, preventing any phase segregation at the nanoscopic scale [27,39,40].

3.3 Generation of Porous Networks from Semi-IPNs

Porous methacrylic networks were obtained by mere extraction of the un-crosslinked oligoesters from oligoester/PMMA (50/50 wt%) semi-IPNs (**Fig. 3**). One such extraction was performed with a good solvent of oligoesters at a temperature (40°C) far below the T_g value of PMMA network to avoid the collapse of the residual porous structures [26,41-43]. The amounts of soluble fractions are reported in Table 5. Regardless of the oligoester nature and molar mass, the extraction of linear oligomers was quantitative as indicated by extractable contents higher than or equal to 50 wt%. Furthermore, ^{1}H NMR and SEC analyses of the soluble fractions showed that they were constituted of more than 95% of oligoester precursor. No undesired grafting of PLA or PCL sub-chains onto PMMA sub-networks through transfer reactions was detected in the present systems. The total disappearance of the characteristicbands associated with α,ω-dihydroxy-oligoester (hydroxyland carbonyl groups) in the FTIR spectra of semi-IPNs afterextraction

confirmed the latter assertion. DSC analyses (**Table 2**) showed that the T_g and ΔC_pvalues of semi-IPNs after extraction matched pretty well those of the correspondingsingle network (**Table 3**). This arose from thequantitative extraction of oligoesters. Nevertheless for PLA 3,700 g.mol^{-1}-based systems,$T_{g,onset}$was slightly lower than the value expected,probably due to a non quantitative extraction as shown also by anextractable content of 48 %.

The morphologiesof semi-IPNs after extraction were examinedby SEM (**Fig.5**).The micrographs revealed highly porous structures, thus showing the effective role of oligoesters as template porogens. Pore sizes strongly depended on the oligoester nature and molar mass. Indeed, pore diameters were as large as 450 nm for PLA-based systems and 1,000 nm for PCL-based-system homologues. Moreover, pore sizes clearly increased when increasing the oligoester molar mass (**Table 7**). The pore size distributions were also determined through DSC-based thermoporometry using water as the penetrant solvent. We already used this technique for the determination of pore size distributions in (semi-)IPNs which also gave complementary results compared to SEM analysis, as thermoporometry allows for the measurement ofthe smallerpore diameters (<200 nm) [26,27]. The pore size ranges are reported in **Table 7** and pore size distributions are shown in **Fig.6a**. Overall, the pore sizes obtained by SEM and those determined by thermoporometry were in reasonable agreement. Finally, the dependence of pore sizes in such porous materialsmirrored the differences observed in semi-IPNprecursors from visual aspects, DSC analysis, and polymer-polymer miscibility inferred from thecalculation of oligoester/PMMA interaction parameters.To conclude, the miscibility of both partners in semi-IPN systems is the most essential parameter controlling the pore size distribution after extraction. Nanoporous structures with poressmaller than 150 nm could be engineeredwhen usinga PLA

oligomer with amolar mass lower than around 2 000 g.mol^{-1}, while a PCL oligomer with the latter molar mass led to a porous structure with a very broad pore size distribution.

Pore volumes of porous networks were obtained through mass swelling ratio in water and led to the determination of apparent density and porosity ratio values (**Table 8**). Porosity ratioswere all around 50 vol% which matched the expected values, taking into account the quantitative extraction of linear oligoesters from semi-IPNs with a 50/50 wt% oligoester/PMMA composition.As also seen in SEM micrographs, this strongly indicated that the porous networks were monolithic structures constituted of open pores or interconnected channels through which a fluid could circulate. Moreover, the porous samples were wrapped in apolyethylene film and placed in *n*-pentane ($d_{20°C}$= 0.624): in such a low-density solvent, they did float,thus confirming apparent density as well as porosityratio values lower than or equal to values around 0.6.

3.4 Engineering Nanoporous Networks from IPNs

Porous networks were produced by an original approach through the total hydrolysis of the polyester sub-network associated with partially hydrolyzable polyester/PMMA (50/50 wt%) IPNs [27,39,40]. Advantage of the contrasted hydrolytic degradability of aliphatic polyesters and PMMA was thus taken. The degradation was conducted for 24 h at 60°C using a 50/50 vol% mixture of methylamine (pH = 13.6) and ethanol. It has to be stressed that the hydrolysis was performed at an intermediate temperature between the T_g of polyester single networks and that of PMMA single network to avoid the collapse of the residual porous methacrylic structures, while allowing for an efficient degradation of the polyester partner. The role of ethanol wasdual: *(i)* increasing the hydrophilic behaviour of the methacrylic sub-network, thusenabling a better diffusion of the medium into the IPN structure [44,45], and *(ii)* increasing the diffusion rate of the degradation products outside the networkas ethanol is a good solvent of oligoesters. With these

conditions, PLA- and PCL-based single networks were completely hydrolyzed after 5 min and 3.5 h, respectively, while no mass loss was detected for 10 mol% DUDMA-based single networks. **Table 5** gives the mass losses obtained after hydrolysis of IPNs. Regardless of the oligoester precursor nature or molar mass, mass loss values close to 50 wt% were determined, which demonstrated a nearly quantitative degradation of the oligoester-derivatized sub-networkfrom polyester/PMMA (50/50 wt%) IPNs. Moreover, the total disappearance of the characteristic bands associated with polyester sub-networks (urethane and carbonyl groups) in the FTIR spectra of residual networks after hydrolysis confirmed their methacrylic structure. Nevertheless, in comparison to the corresponding PMMA single network, the residual methacrylic networks, after IPN hydrolysis, exhibited a low intensity band from 3,700 cm^{-1} to 2,300 cm^{-1} and a band at 1,660 cm^{-1}. This showed the appearance of carboxylic acid groups due to the partial hydrolysis of ester groups of the PMMA sub-network. Furthermore, the $T_{g,onset}$ values of IPNs after hydrolysis (see **Table 6**) were higherthan that of the corresponding PMMA single network (*i.e.*, 118°C). As no mass loss was detected for thissingle network, it was possible to hypothesize that the partial hydrolysis of PMMA sub-network was essentially due to the hydrolysis of ester side groups in the PMMA sub-chains without degrading the main chain and cross-linking points.

The morphologies of typicalIPNs after hydrolysis were examined by SEM (**Fig. 7**).It was difficult to obtain images with a good resolution without degrading the materials during the SEM analysis. Nevertheless, it is noteworthy that the residual networks typically exhibitednanoporous structures with pore sizessmaller than 100 nm. With such materials, the thermoporometry technique was very useful to determine pore sizes and the pore size distributions. The pore size ranges thus obtained are reported in **Table 7**, and pore size distributions are shown in **Fig.6b**.Pore sizes were always smaller than 150nm, and thisresult mirrored the observations made from visual

aspectsof IPNprecursors. As expected, compared to semi-IPN analogues, the pore diameters were dramatically decreased due to the good chain interpenetration of both polyester and PMMA sub-networks in the interlocking framework of IPN precursors. Moreover, as already hypothesized from DSC analysis, the pore size increased with the oligoester precursor molar mass, but no differences were noticed between PLA- and PCL-based IPN precursors. This meant that domain sizes in IPNs were larger when the cross-linking density of the polyester sub-network was smaller, regardless of the miscibility between PLA/PCL and PMMA. This result was in a good agreement with literature reports [25,46,47]. As a matter of fact, when synthesizing IPNs by the sequential method, the network first formed constitutes the most continuous phase, and its cross-linking density generally determines the final morphology of the system, while the cross-linking density of the second network has no significant effect.

Pore volumes of nanoporous networks were obtained through mass swelling measurements in water and led to the determination of the apparent density and the porosity ratio values (**Table 8**).Porosity ratios ranged from 33 to 42%, which was lower than expected values, taking into account the quantitative hydrolysis of polyester sub-network from polyester/PMMA (50/50 wt%) IPNs. This was probably due to a partial collapse of the resulting porous structures. Porosity ratio increasedwith the oligoester precursor molar mass,due tolarger pore sizes.

4 Conclusions

This contribution highlights the effectiveness and versatility of using oligoester-derivatized semi-IPNs and IPNs as nanostructured precursors to porous networks with tunable porosity.Miscellaneous PLA- or PCL-containing methacrylic (semi-)IPNs were indeed prepared

as model systems from corresponding oligomers with different molar masses, and the pore sizes of related porous materials could be correlated with the polyester domain sizes inferred from the physico-chemical analysis of the (semi-)IPN precursors. Even though the quantitative extraction of uncrosslinked oligoestersfrom semi-IPNs generally led to the formation of macroporous networks, the semi-IPN approach constituted a straightforward and effective route toward nanoporous networks provided the extent of miscibility between both semi-IPN partners was high, *i.e*. when using the lower molar mass oligoester and preferably PLA. Alternatively, the complete hydrolysis of the polyester sub-networkfrom IPNs afforded more versatility, since nanoporous networks were generally derived therefrom, regardless of the molecularfeatures associated with the oligoesters. The nanoporosity of residual porous networks could be attributed to the good degree of chain interpenetration associated with both sub-networks in IPN precursors arising from their peculiar interlocking framework. Still, pore sizes in nanoporous frameworks increased with increasing oligoester molar masses, as the extent of microphase separation in IPNs was larger when the crosslinking density of polyester sub-network decreased.

Such complementary routes involving semi-IPN and IPN systems may provide a straightforward and facile means to tune the morphology associated with (nano-)porous polymeric materials. Moreover, the functionalization of the pore surface through the initial incorporation of functional monomers in the (semi-)IPNs precursors may allow for the development ofa large variety of applications mainly expected in the areas of separation techniques (chromatographic supports, selective membranes) and chemistry in confined media (nanoreactors, catalytic supports).

Conflict of interest statement

On behalf of all authors, the corresponding author states that there is no conflict of interest.

1

References

[1] Buchmeiser MR (2001) Angew Chem Int Ed 40:3795.

[2] Sykora D, Peters EC,Svec F, Fréchet JMJ (2000) Macromol Mater Eng 275:42.

[3] Hentze HP, Antonietti M. (2002) Rev Mol Biotech 90:27.

[4] Dauben M, Reichert KH, Huang P, Fock J (1996) Polymer 37:2827.

[5] Allender CJ, Richardson C, Woodhouse B, Heard CM, Brain KR (2000) Int J Pharm 195:39.

[6] Byrne ME, Oral E, Hilt JZ, Peppas NA (2002) Polym Adv Technol 13:798.

[7] Cameron NR (2004) Polymer 46:1439.

[8] Poupart R, Benlahoues A, Le Droumaguet B,Grande D (2017) ACS Appl Mater Interfaces 9:31279.

[9] Balaji R, Boileau S, Guérin P, Grande D (2004) Polym News 29:205.

[10] Wu D, Xu F, Sun B, Fu R, He H, Matyjaszewski K (2012) Chem Rev 112:3959.

[11] Kayaman-Apohan N, Baysal BM (2001) Macromol Chem Phys 202:1182.

[12] Widmaier JM, Sperling LH (1982)Macromolecules 15:625.

[13] Widmaier JM, Sperling LH (1984) Br Polym J 16: 46.

[14] Du Prez F, Goethals EJ (1995) Macromol Chem Phys 196:903.

[15] De Clercq RR, Goethals EJ (1992)Macromolecules 25:1109.

[16] Hu J, Pompe G, Schulze U, Pionteck J. (1998)Polym Adv Technol 9:746.

[17] Hu J, Schulze U Pionteck J (1999) Polymer 40:5279.

[18] Pionteck J, Hu J, Schulze U (2003) J Appl Polym Sci 89:1976.

[19] Sperling LH (1981) Interpenetrating Polymer Networks and Related Materials. Plenum Press, New York.

[20] Sperling LH (1988) In:Comprehensive Polymer Science. Pergamon Press, New York, Vol. 6, pp. 423-436.

[21] Sperling LH, Mishra V (1996)Polym Adv Technol7:197.

[22] Kim SC, Sperling LH (1997) IPNs Around the World: Science and Engineering. Wiley, Chichester, UK.

[23] Athawale VD, Kolekar SL, Raut SS (2003) J Macromol Sci Part C: Polym RevC43:1.

[24] Thomas S, Grande D, Cvelbar U, Raju KVSN, Narayan R, Thomas S, Akhina H (2016) Micro- and Nano-Structured Interpenetrating Polymer Networks: From Design to Applications. John Wiley & Sons, Hoboken, NJ.

[25] Dean K, Cook WD (2002)Macromolecules35:7942.

[26] Rohman G, Grande D, Lauprêtre F, Boileau S, Guérin P (2005)Macromolecules 38:7274.

[27] Rohman G, Lauprêtre F, Boileau S, Guérin P, Grande D (2007) Polymer 48:7017.

[28] Bachari A, Bélorgey G, Hélary G, Sauvet G (1995) Macromol Chem Phys 196:411.

[29] Brun M, Lallemand A, Quinson JF, Eyraud C. (1977)Thermochim. Acta 21:59.

[30] Iza M, Woerly S, Danumah C, Kaliaguine S, Bousmina M (2000) Polymer 41:5885.

[31] HayJN, Laity PR (2000)Polymer 41:6171.

[32] Rabelo D, Coutinho FMB (1993) Polym Bull 30:725.

[33] Okay O (2000)Prog Polym Sci 25:711.

[34] Eguiburu JL, Iruin JJ, Fernandez-Berridi MJ, San Roman J (1998) Polymer39:6891.

[35] Klein PG, Ebdon JR, Hourston DJ (1988) Polymer29:1079.

[36] Grulke EA (1999) In:Brandrup J, Immergut EH, Grulke EA (eds)Polymer Handbook, 4th Ed. Wiley-Interscience, New York,p. VII/679.

[37] Coleman MM, Serman CJ, Bhagwagar DE, PainterPC (1990)Polymer 31:1187.

[38] Van Krevelen DW (1997) Properties of Polymers. Elsevier, Amsterdam.

[39] Majdoub R, Dirany M, Benzina M, Grande D (2013) Matériaux & Techniques 101:405.

[40] Grande D, Beurroies I, Denoyel R (2010) Macromol Symp 291:168.

[41] Grande D, Rohman G, Millot MC (2008)Polym Bull 61:129.

[42] Lav TX, Carbonnier B, Guerrouache M,Grande D (2010)Polymer 51:5890.

[43] Lav TX,Grande D, Gaillet C,Guerrouache M, Carbonnier B (2012)Macromol Chem Phys 213:64.

[44] Yan J, Wang XH, Chen J (2000)J Appl Polym Sci75:536.

[45] Wei J, Bai XY, Yan J (2003)Macromolecules36:4960.

[46] Donatelli AA,Sperling LH, Thomas DA (1976)Macromolecules9:671.

[47] Hourston DJ, Schäfer FU (1996)Polymer37:3521.

Table 1 Molecular and thermal characteristics of oligoesters

Nature	M_n[a] (g.mol^{-1})	$Đ$[b]	T_g[c] (°C)	ΔC_p[d] (J.g^{-1}.°C^{-1})	T_m (°C)	ΔH_m (J.g^{-1})	X_c[e] (%)
PLA	570	1.2	-20	0.57	-	-	-
	1,700	1.2	10	0.55	-	-	-
	3,700	1.4	25	0.61	-	-	-
PCL	560	1.7	-80	0.16	36	46.1	34
	2,100	2.1	-70	0.35	65	89.7	66

[a]Molar mass as determined by ^{1}H NMR. [b]Polydispersity index as determined by SEC in THF with polystyrene standards for calibration. [c]$T_g$value as obtained at the midpoint. [d]$\Delta C_p = C_{p,v} - C_{p,g}$: heat capacity jump at T_g as determined by DSC, where C_p is the heat capacity, the subscripts v and g refer to the "viscous" and "glassy" states, respectively. [e] crystallinity degree calculated with ΔH_{m0}(100 % crystalline PCL) = 135 J.g^{-1}.[Kweon HY, Yoo MK, Park IK, Kim TH, Lee HC, Lee HS, Oh JS, Akaike T, Cho CS (2003) Biomaterials 24:801]

Table 2 Visual aspect and DSC analysis of semi-IPNs before and after extraction

Oligoester nature and molar mass	Visual aspect [a]	Semi-IPNs before extraction			Semi-IPNs after extraction		
		$T_{g\ onset}$ (°C)	ΔT_g [b] (°C)	ΔC_p [c] ($J.g^{-1}.°C^{-1}$)	$T_{g,onset}$ (°C)	ΔT_g [b] (°C)	ΔC_p [c] ($J.g^{-1}.°C^{-1}$)
PLA 570 $g.mol^{-1}$	tr	-14	25	0.25	116	25	0.24
PLA 1,700 $g.mol^{-1}$	tl	25	18	0.23	116	27	0.19
PLA 3,700 $g.mol^{-1}$	o	39	13	0.19	106	31	0.23
PCL 560 $g.mol^{-1}$	tl	-70 (T_m = 38°C, ΔH_m = 22.2 $J.g^{-1}$, X_c [d] = 16%)	40	0.05	112	31	0.17
PCL 2,100 $g.mol^{-1}$	o	-65 (T_m = 63°C, ΔH_m = 40.0 $J.g^{-1}$, X_c [d] = 30%)	38	0.18	117	25	0.18

[a] o: opaque, tl: translucent, tr: transparent. [b] $\Delta T_g = T_{g,end} - T_{g,onset}$: range of temperatures in which the glass transition occurs as determined by DSC. [c] $\Delta C_p = C_{p,v} - C_{p,g}$: heat capacity jump at T_g as determined by DSC, where C_p is the heat capacity, the subscripts v and g refer to the "viscous" and "glassy" states, respectively. [d] crystallinity degree calculated with ΔH_{m0}(100% crystallinePCL) = 135 $J.g^{-1}$.[Kweon HY, Yoo MK, Park IK, Kim TH, Lee HC, Lee HS, Oh JS, Akaike T, Cho CS (2003) Biomaterials 24:801]

Table 3 DSC analysis of polyester and PMMA single networks

	Oligoester nature and molar mass	$T_{g,onset}$ **(°C)**	ΔT_g [a] **(°C)**	ΔC_p [b] **(J.g^{-1}.°C^{-1})**
Polyester single networks	PLA 570 g.mol^{-1}	50	30	0.32
	PLA 1,700 g.mol^{-1}	20	25	0.29
	PLA 3,700 g.mol^{-1}	30	15	0.27
	PCL 560 g.mol^{-1}	-5	25	0.28
	PCL 2,100 g.mol^{-1}	-55 (T_m = 50 °C, ΔH_m = 4 J.g^{-1})	10	0.32
PMMA single network	-	118	19	0.16

[a] $\Delta T_g = T_{g,end} - T_{g,onset}$: range of temperatures in which the glass transition occurs as determined by DSC. [b] $\Delta C_p = C_{p,v} - C_{p,g}$: heat capacity jump at T_g as determined by DSC, where C_p is the heat capacity, the subscripts v and g refer to the "viscous" and "glassy" states, respectively.

Table 4 Variations of χ_{cr} with oligoester nature and molar mass for 10 mol% DUDMA-based systems

Oligoester nature and molar mass	χ_{cr}
PLA 570 $g.mol^{-1}$	0.32 ± 5.10^{-3}
PLA 1,700 $g.mol^{-1}$	0.21 ± 5.10^{-3}
PLA 3,700 $g.mol^{-1}$	0.17 ± 5.10^{-3}
PCL 560 $g.mol^{-1}$	0.34 ± 5.10^{-3}
PCL 2,100 $g.mol^{-1}$	0.24 ± 5.10^{-3}

Table 5 Soluble fractions associated with single networks and polyester/PMMA (50/50 wt%) (semi-)IPNsafter extraction as well asmass loss associated with polyester/PMMA (50/50 wt%) IPNs after hydrolysis [a]

Oligoester nature and molar mass	Soluble fractions after extraction (wt%)				Mass loss (wt%) after IPN hydrolysis
	Polyester single networks	PMMA single networks	Semi-IPNs	IPNs	
PLA 570 $g.mol^{-1}$	9	-	53	11	46
PLA 1,700 $g.mol^{-1}$	6	-	51	10	47
PLA 3,700 $g.mol^{-1}$	5	-	48	23	48
PCL 560 $g.mol^{-1}$	11	-	50	11	48
PCL 2,100 $g.mol^{-1}$	12	-	56	14	49
-	-	3	-	-	-

[a]Experimental conditions: $[DBTDL]_0/[Oligoester]_0$=0,44 - $[NCO]_0/[OH]_0$ = 1,4 –MMA/DUDMA molar ratio: 90/10 - $[AIBN]_0/([MMA]_0 + 2[DUDMA]_0)$ = 0.02 –20h at room T (only for polyester single networks and IPNs)+ 2h at 65°C + 2h at 110°C.

Table 6 DSC analysis of IPNs before and after hydrolysis

Oligoester nature and molar mass	IPNs before hydrolysis			IPNs after hydrolysis		
	$T_{g,onset}$ (°C)	ΔT_g [a] (°C)	ΔC_p [b] ($J.g^{-1}.°C^{-1}$)	$T_{g,onset}$ (°C)	ΔT_g [a] (°C)	ΔC_p [b] ($J.g^{-1}.°C^{-1}$)
PLA 570 $g.mol^{-1}$	58	35	0.26	122	23	0.21
PLA 1,700 $g.mol^{-1}$	45	46	0.22	128	16	0.15
PLA 3,700 $g.mol^{-1}$	45	49	0.22	126	19	0.21
PCL 560 $g.mol^{-1}$	38	32	0.23	121	15	0.19
PCL 2,100 $g.mol^{-1}$	-50	52	0.14	126	20	0.19

[a] $\Delta T_g = T_{g,end} - T_{g,onset}$: range of temperatures in which the glass transition occurs as determined by DSC. [b] $\Delta C_p = C_{p,v} - C_{p,g}$: heat capacity jump at T_g as determined by DSC, where C_p is the heat capacity, the subscripts v and g refer to the "viscous" and "glassy" states, respectively.

Table 7 Pore diameters of resulting porous networksafter extraction of semi-IPNs orhydrolysis of IPNs as determined by SEM and DSC-based thermoporometry

Oligoester nature and molar mass	**Pore diameters**		
	Semi-IPNs		**IPNs**
	SEM (nm)	DSC (nm)	DSC (nm)
PLA 570 $g.mol^{-1}$	10-75	40-115	17-75
PLA 1,700 $g.mol^{-1}$	25-150	30-140	20-80
PLA 3,700 $g.mol^{-1}$	75-450	10-200 [a]	30-150
PCL 560 $g.mol^{-1}$	25-150	50-170	20-65
PCL 2,100 $g.mol^{-1}$	150-1,000	10-200 [a]	20-95

[a]DSC-based thermoporometry only allowed for determination of pore size up to 200 nm. For larger pore sizes, the melting peaks of confined and bulk water were not resolved: confined water just behaved as a bulk solvent.

Table 8 Pore volume (V_{pore}), apparent density (d_{app}), and porosity ratio (P) of resulting porousnetworks after extraction of semi-IPNs or hydrolysis of IPNs

Oligoester nature and molar mass	**Semi-IPNs**			**IPNs**		
	V_{pore} ($cm^3.g^{-1}$)	d_{app}	P	V_{pore} ($cm^3.g^{-1}$)	d_{app}	P
PLA 570 $g.mol^{-1}$	0.87	0.59	0.51	0.42	0.80	0.33
PLA 1,700 $g.mol^{-1}$	0.89	0.58	0.52	0.55	0.72	0.40
PLA 3,700 $g.mol^{-1}$	0.86	0.59	0.51	0.54	0.72	0.40
PCL 560 $g.mol^{-1}$	0.84	0.59	0.50	0.42	0.79	0.34
PCL 2,100 $g.mol^{-1}$	0.83	0.60	0.50	0.60	0.69	0.42

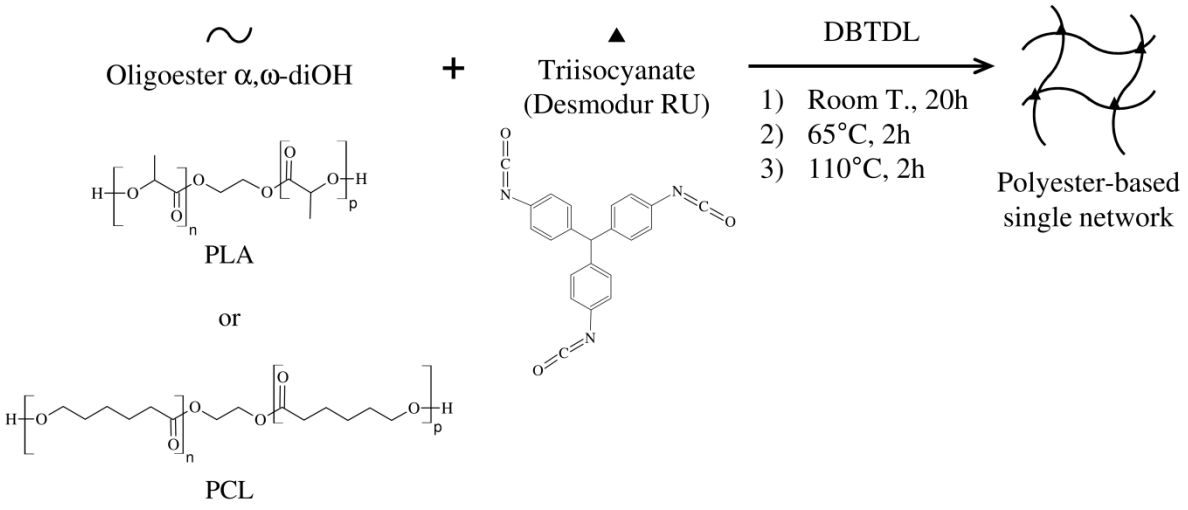

Fig. 1 Preparation of polyester-based single networks

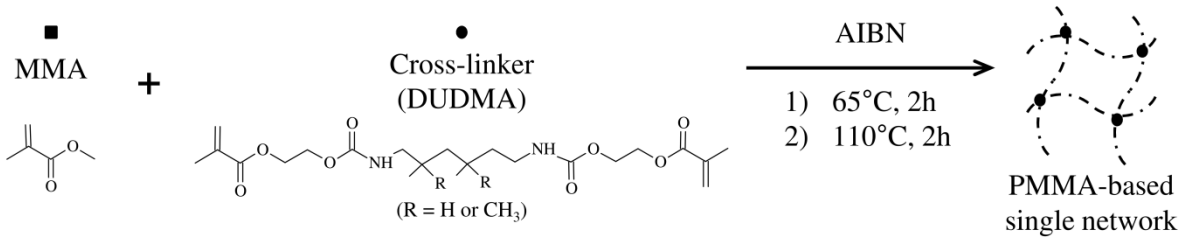

Fig. 2 Preparation of PMMA-based single networks

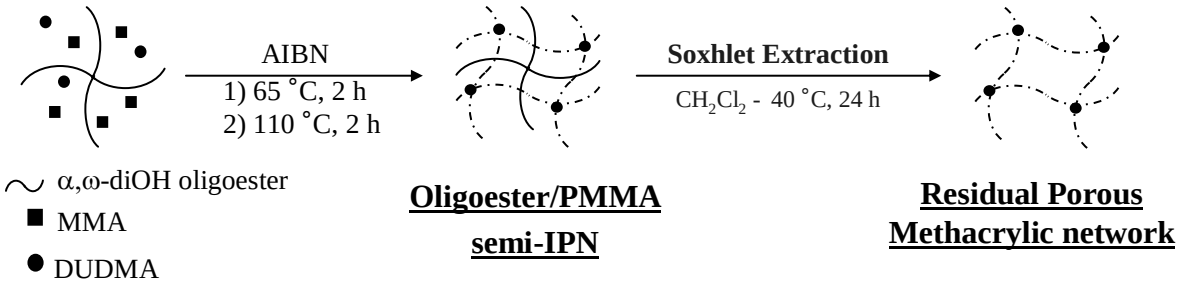

Fig.3 Synthesis of oligoester/PMMA-based semi-IPNs and design of porous PMMA networks derived therefrom

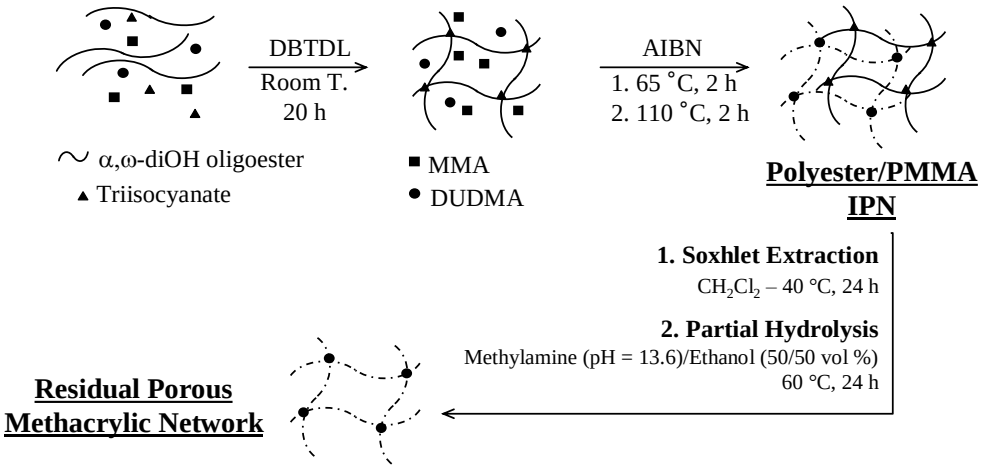

Fig.4 Synthesis of polyester/PMMA-based IPNs and design of porous methacrylic networks derived therefrom

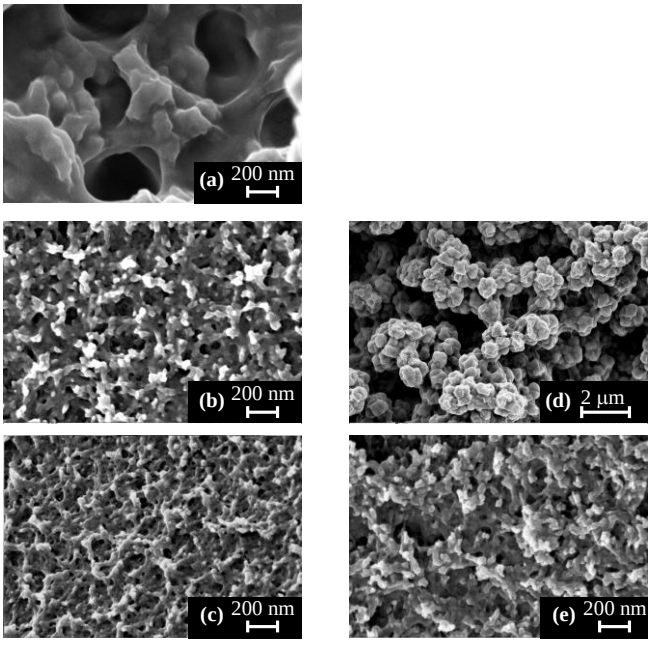

Fig. 5 SEM micrographs of porous networks derived from extraction of oligoester/PMMA (50/50 wt%) semi-IPNs:PLA-based systems: (a) 3,700 g.mol^{-1}, (b) 1,700 g.mol^{-1}, (c) 560 g.mol^{-1};PCL-based systems: (d) 2,100 g.mol^{-1}, (e) 570 g.mol^{-1}

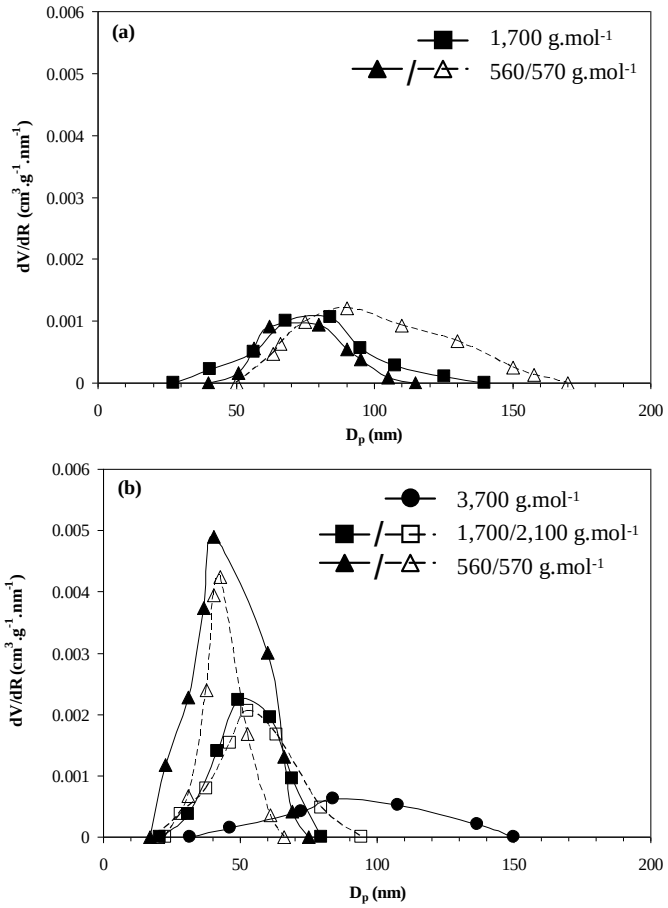

Fig. 6 Pore size distribution profiles of porous methacrylic networks as determined by DSC-based thermoporometry for PLA- (full symbols) and PCL- (empty symbols) containing systems with varying oligoester molar masses: (a) semi-IPNs after extraction, (b) IPNs after hydrolysis

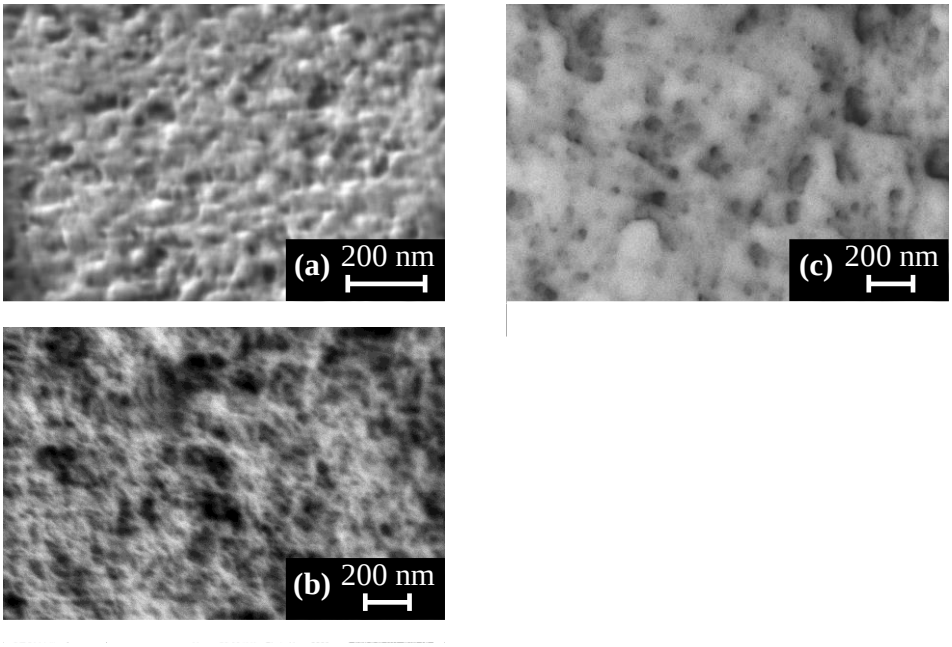

Fig. 7 SEM micrographs of porous networks derived from partial hydrolysis of polyester/PMMA (50/50 wt%) IPNs:PLA-based systems: (a) 1,700 $g.mol^{-1}$, (b) 560 $g.mol^{-1}$;PCL-based systems: (c) 2,100 $g.mol^{-1}$